

# A simple and precise method for the threshold current determination in vertical-cavity surface-emitting lasers

EMILIA PRUSZYŃSKA-KARBOWNIK<sup>1\*</sup>, MARCIN GĘBSKI<sup>1,2</sup>, MAGDALENA MARCINIAK<sup>1,2</sup>,  
JAMES A. LOTT<sup>2</sup>, TOMASZ CZYSZANOWSKI<sup>1</sup>

<sup>1</sup>Institute of Physics, Lodz University of Technology, Wólczańska 219, 90-924 Łódź, Poland

<sup>2</sup>Institute of Solid State Physics and Center of Nanophotonics, Technische Universität Berlin,  
Hardenbergstraße 36, Berlin, Federal Republic of Germany

\*Corresponding author: emilia.pruszyńska-karbownik@p.lodz.pl

In this paper, we present experimental results of spontaneous emission clamping in the threshold for vertical-cavity surface-emitting lasers (VCSELs) with oxide current confinement. We show that the spontaneous emission not wholly clamps in the threshold. We propose a new method for determining the threshold current value using the study of the clamping phenomena. This method has an advantage over the commonly used methods in the accuracy because the current of the spontaneous emission clamping is better defined than the current of the slope change of the stimulated emission light-current curve. The estimated uncertainty of the method is no more than 20  $\mu\text{A}$ .

Keywords: VCSEL, threshold current, spontaneous emission.

## 1. Introduction

The threshold current is one of the most important parameters of semiconductor lasers. The determination of its value is crucial for the assessment of thermal properties, quality of performance, and the applicability of the laser devices. Although the threshold current is a basic quantity and is intuitively easy to understand, it is defined in several ways. As a first example, the threshold is defined as a state in which the gain in the active region of the laser compensates all the cavity and mirror losses [1, 2]. However, BJÖRK *et al.* show that this definition fails in the case of lasers with small cavities, and they propose the definition of the threshold as a state in which the mean number of photons in the cavity is equal to one [3]. The quantities used for the threshold definitions are difficult to determine experimentally. Therefore, the measurement methods are mainly based not on the threshold definition but its practical consequences. The threshold definition is also beyond the scope of our paper.

The practical measurement methods to determine the threshold current include: a sudden increase of the emitted optical output power, a sudden narrowing of the emission spectrum, a sudden spatial narrowing of the laser beam [4], the resonance of the

autocorrelation function in small-signal modulation [5], and the dependence of the forward bias current ( $y$ -axis) *versus* the square of the relaxation resonance oscillation frequency ( $x$ -axis) where the  $y$ -axis intercept is taken as the threshold current [6]. However, the first of these methods is the method most used in practice. This is because the threshold current is determined based on light-current ( $L$ - $I$ ) curves, and the measurement requires only a power supply and a photodetector. Unfortunately, the  $L$ - $I$  curves for diode lasers are smooth in the threshold region and the threshold current can only be estimated. This is especially the case for vertical-cavity surface-emitting lasers (VCSELs), because of their small resonant cavity length and high spontaneous emission factor [7–9].

In addition to the phenomena mentioned earlier, another symptom of the threshold is clamping of the spontaneous emission. It is usually assumed that above the threshold, the carrier density in the active region is constant because stimulated recombination consumes all excess carriers. Therefore, the gain and the spontaneous emission intensity above the threshold should be constant [1]. However, PAOLI showed that in semiconductor lasers, for wavelengths higher than the lasing wavelength, the spontaneous emission does not sharply clamp [10].

Although the spontaneous emission in VCSELs is still the subject of active debate and research [11, 12] and the clamping phenomenon is often used in VCSEL modelling [13], no measurement results of the spontaneous emission over the threshold in these lasers have been published to date. In this paper, we present the first experimental study of the clamping phenomenon in VCSELs and we propose a practical and fast method to determine the threshold current based on this phenomenon.

## 2. Experiment

### 2.1. VCSEL structure

For the experiment, we made GaAs-based VCSELs designed for emitting near-infrared light with a peak wavelength of 980 nm. The active region consists of five 4-nm-thick  $\text{In}_{0.2}\text{Ga}_{0.8}\text{As}$  quantum wells alternated with six 5 nm-thick  $\text{GaAs}_{0.9}\text{P}_{0.1}$  barrier layers. The active region is sandwiched between 16.5 periods of the C-doped p-type  $\text{Al}_{0.9}\text{Ga}_{0.1}\text{As}/\text{GaAs}$  distributed Bragg reflector (DBR) and 35 periods of the Si-doped n-type  $\text{Al}_{0.9}\text{Ga}_{0.1}\text{As}/\text{GaAs}$  DBR. Four 20-nm-thick oxide-aperture layers located in nodes in the p-type DBR confine the electrical current in the active region. The depth of the oxidations in the exposed top mesa sidewalls is about 23  $\mu\text{m}$ . Information about the fabrication technology can be found in [14].

In the experiment, we measured lasers with three different mesa diameters and, thus, three different current oxide apertures. The oxide aperture diameters are 2, 12, and 16  $\mu\text{m}$ .

### 2.2. Measurement set-up

We measured the optical output power *versus* current ( $L$ - $I$ ) characteristics of the lasers in two configurations of the experimental set-up. In the first configuration, named the

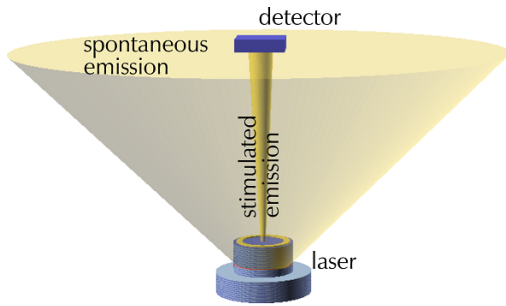


Fig. 1. Design of the experimental set-up in the on-axis configuration.

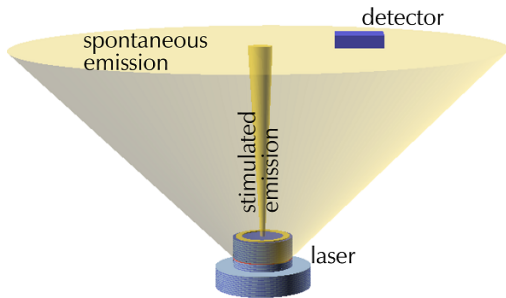


Fig. 2. Design of the experimental set-up in the off-axis configuration.

on-axis configuration, the detector is centred on the laser beam axis (see Fig. 1) and the distance between the laser and the detector is 6 mm. In the second configuration, named the off-axis configuration, the photodetector is placed outside the laser beam to detect the sidelight electroluminescence which is spontaneous emission (see Fig. 2). The detector is placed on the same height as in the on-axis configuration. The angle between the beam propagation direction and the laser photodetector line is about  $60^\circ$ .

In both configurations, the laser is supplied by a continuous current source (Thorlabs LDC8005 PRO8000), the radiation is detected by a silicon photodiode (Thorlabs S130C), and the current value is measured by an external multimeter (Keithley 2000). The resolution of the optical power measurement is 100 pW and the resolution of the power supply current measurement is 10 nA. The measurements are performed at several temperatures in the range of 288–343 K.

### 2.3. Methods of threshold current determination based on light-current curves

There are four widely used methods for the estimation of the threshold current based on the  $L$ - $I$  curves including: 1) the linear line fit method; 2) the two-segment line fit method; 3) the first derivative method; 4) the second derivative method.

*Linear line fit method* [1, 11]. In this method, only the over-threshold part of the  $L$ - $I$  curve is taken into consideration. The threshold current is determined as a point

of the intersection of the linear line fit of the over-threshold  $L-I$  curve with the current axis. This is the simplest and the most commonly used method.

*Two-segment line fit method* [11]. In this method, two linear fits are used: one fit of the over-threshold  $L-I$  curve (like in the linear line fit method) and the fit of the under-threshold curve. The threshold current is determined as a point of the intersection of these lines.

*First derivative method* [1, 11]. In this method, the derivative of the optical output power over the current is calculated. The threshold current is determined as a current in which the derivative reaches half of its maximum value. This method requires prior smoothing of the  $L-I$  curves.

*Second derivative method* [8, 11]. In this method, the second derivative of the optical output power over the current is calculated. The threshold current is determined as a current in which the second derivative reaches its maximum value. This method is considered the most accurate, and also requires prior smoothing of the  $L-I$  curves.

In this paper, we propose another method, based on finding a *kink of the off-axis  $L-I$  curve*. In this method, two linear fits are used, as in the two-segment line fit method, but the fitted curve is the spontaneous-emission power *versus* current curve.

### 3. Results

Figures 3, 4, and 5 show measured  $L-I$  curves of the lasers with 2, 12, and 16  $\mu\text{m}$  oxide aperture diameters, respectively. The beam of the 2- $\mu\text{m}$  VCSEL is single-transverse-mode beam while the beams of the other two are multi-transverse-mode beams. Optical output power values measured in the off-axis configuration of the set-up are multiplied by constant values to normalize the below-threshold part of the off-axis curves to the on-axis curve.

Based on the on-axis measurements, we determine the values of the threshold current by using the four different methods described in Section 2.3. The Table presents these values for the ambient temperature of 288 K compared with the current values

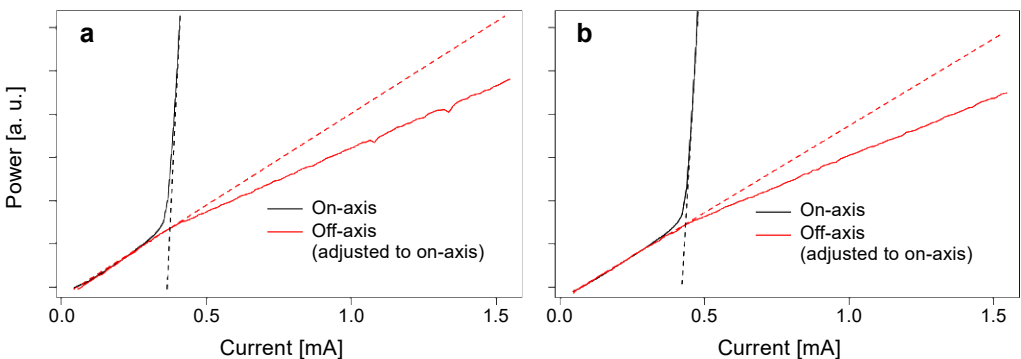


Fig. 3. Light-current curves measured for a VCSEL with a 2- $\mu\text{m}$  oxide aperture diameter in two ambient temperatures: 288 K (a) and 343 K (b). The dashed lines are extrapolations of the linear parts of the on-axis curve.

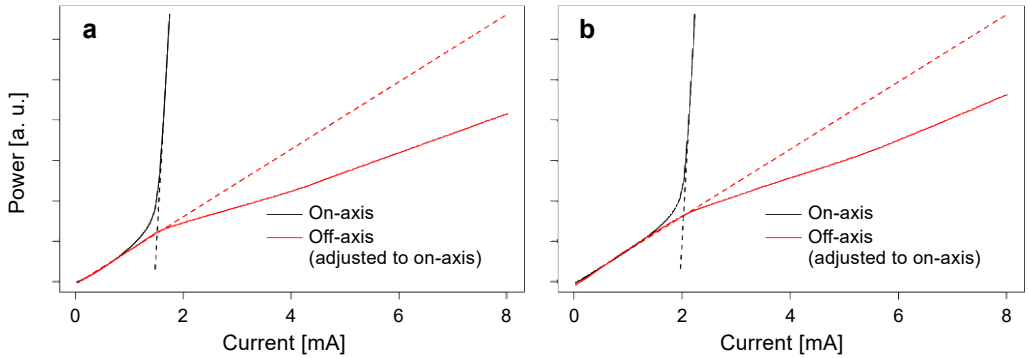


Fig. 4. Light-current curves measured for a VCSEL with a 12- $\mu\text{m}$  oxide aperture diameter in two ambient temperatures: 288 K (a) and 343 K (b). The dashed lines are extrapolations of the linear parts of the on-axis curve.

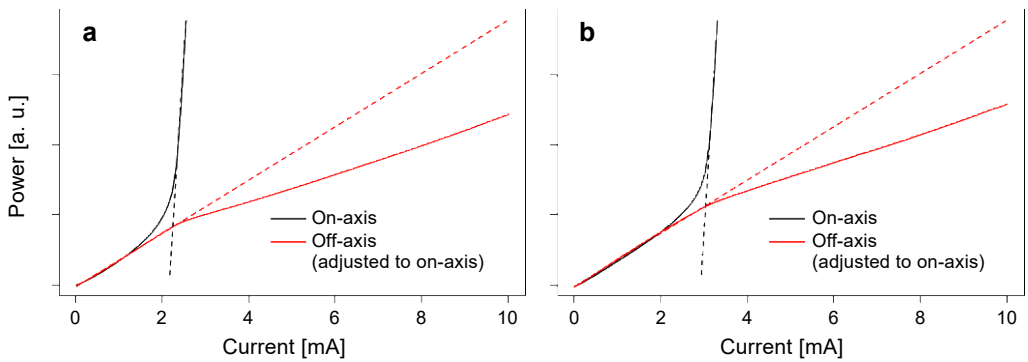


Fig. 5. Light-current curves measured for a VCSEL with 16- $\mu\text{m}$  oxide aperture diameter in two ambient temperatures: 288 K (a) and 343 K (b). The dashed lines are extrapolations of the linear parts of the on-axis curve.

T a b l e. Threshold current values in 288 K obtained by various methods.

	Oxide aperture diameter [ $\mu\text{m}$ ]		
	2	12	16
Linear line fit [mA]	0.368	1.547	2.317
Two-segment line fit [mA]	0.378	1.597	2.392
First derivative method [mA]	0.376	1.548	2.339
Second derivative method [mA]	0.377	1.551	2.338
Kink of the off-axis curve [mA]	0.375	1.612	2.442

corresponding with the kinks in the off-axis curves. For small aperture (2  $\mu\text{m}$ ), the linear line fit method gives 2% smaller value of threshold current than the value obtained from the off-axis measurement. Other methods give more converged values, higher than the off-axis value by less than 1%. For wider apertures, all values obtained by these methods are understated in comparison to kink of the off-axis curve. The differ-

ence is 4–5% for the linear line method, 1–2% for the two-segment line fit method and 4% for both derivation methods. The hardware inaccuracies of the power and current measurements are so low compared to the differences between the results that in our measurement they practically do not affect the accuracy of the threshold current determination.

As expected, we observed that on-axis curves are smooth in the threshold region. Based on the dependence of the second derivative on the current, we determined the current range of the light-current curve non-linearity as 0.0864 mA for the 2- $\mu\text{m}$  oxide aperture diameter VCSEL, 0.475 mA for the 12- $\mu\text{m}$  oxide aperture diameter VCSEL, and 0.603 mA for the 16- $\mu\text{m}$  oxide aperture diameter VCSEL. These are, respectively, 23%, 29%, and 25% of the estimated threshold current values. The off-axis curves have sharp slope reduction in the threshold and such a region of non-linearity is smaller than the current step. In the plot of the second derivative for the narrower aperture (see Fig. 6a), the peak corresponding to the threshold current is indistinguishable from noise, but for the wider apertures (see Figs. 6a and 6b) there are one-point-wide negative peaks, low but distinguishable. That means the accuracy of the determination of the kink position (and thus the threshold current) in our experiment is less than twice the current step, *i.e.* 20  $\mu\text{A}$ .

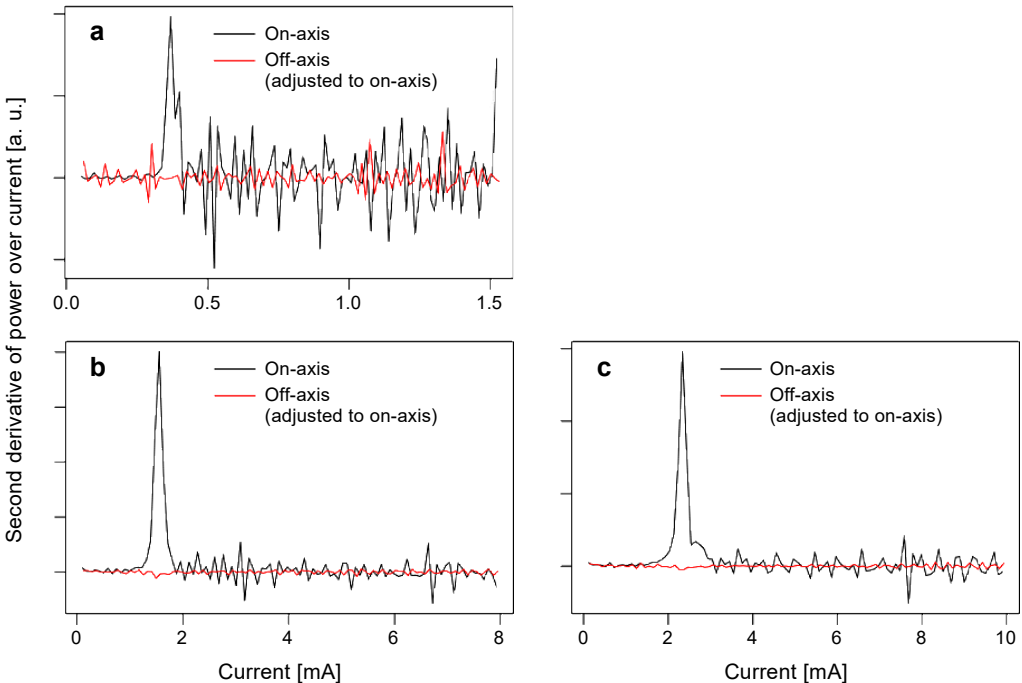


Fig. 6. Plots of the second derivative of power over current determined for VCSELs with 2- $\mu\text{m}$  (a), 12- $\mu\text{m}$  (b) and 16- $\mu\text{m}$  (c) oxide aperture diameter in 288 K. The values determined in the off-axis configuration are multiplied by the same constant values as in Figs. 3, 4, and 5.

For a 2- $\mu\text{m}$  oxide aperture diameter, the slope of the over-threshold curve measured in the off-axis set-up configuration is 0.65 of the below-threshold slope. For 12- $\mu\text{m}$  oxide aperture diameter and 16- $\mu\text{m}$  oxide aperture diameter VCSELs, this ratio is 0.45 and 0.48, respectively.

## 4. Conclusions

The measurements in the off-axis configuration show that in VCSELs the spontaneous emission clamps at the threshold current. However, the clamping is not absolute, and it is stronger for larger oxide aperture diameters and weaker for the smallest oxide aperture diameter. It could be caused by mixing radiation with different wavelengths: lasing wavelength with the sharp clamping and higher wavelengths with soft clamping, as presented by PAOLI for double-heterostructure lasers [10]. To resolve this, spectral measurements must be made.

Unlike the on-axis  $L$ - $I$  curves, the off-axis curves have a sharp kink in the threshold region. This allows for a more accurate threshold current determination based on the off-axis measurements compared with measurements based on standard (on-axis)  $L$ - $I$  curves. We showed that the threshold current values estimated based on standard  $L$ - $I$  curves are understated, which is consistent with conclusions published by KANE and TOOMEY [6]. The shapes of all the  $L$ - $I$  curves in the threshold region do not change with the temperature.

The herein presented method of threshold current determination is as simple as the standard measurement of light-current characteristics but more precise, especially in the case of multi-transverse-mode beams. We estimated the uncertainty of the method at no more than 20  $\mu\text{A}$  and can be even better for a smaller current step. Such accuracy can be useful in particular for determining thermal properties of the lasers, where several threshold current measurements are made.

Furthermore, the method is not phenomenological, but it is based on laser physics – on the occurrence of spontaneous emission clamping at the threshold.

*Acknowledgements* – This work is supported by the Polish National Science Centre grant No. 2015/18/E/ST7/00572

## References

- [1] COLDREN L.A., CORZINE S.W., *Diode Lasers and Photonic Integrated Circuits*, Wiley, 1995.
- [2] MOCK A., *First principles derivation of microcavity semiconductor laser threshold condition and its application to FDTD active cavity modeling*, Journal of the Optical Society of America B **27**(11), 2010, pp. 2262–2272, DOI: [10.1364/JOSAB.27.002262](https://doi.org/10.1364/JOSAB.27.002262).
- [3] BJÖRK G., KARLSSON A., YAMAMOTO Y., *Definition of a laser threshold*, Physical Review A **50**(2), 1994, pp. 1675–1680, DOI: [10.1103/PhysRevA.50.1675](https://doi.org/10.1103/PhysRevA.50.1675).
- [4] SIEGMAN A.E., *Lasers*, University Science Books, 1986.
- [5] WANG T., PUCCIONI G.P., LIPPI G.L., *Onset of lasing in small devices: the identification of the first threshold through autocorrelation resonance*, Annalen der Physik **530**(8), 2018, article 1800086, DOI: [10.1002/andp.201800086](https://doi.org/10.1002/andp.201800086).

- [6] KANE D.M., TOOMEY J.P., *Precision threshold current measurement for semiconductor lasers based on relaxation oscillation frequency*, Journal of Lightwave Technology **27**(15), 2009, pp. 2949–2952, DOI: [10.1109/JLT.2009.2019112](https://doi.org/10.1109/JLT.2009.2019112).
- [7] MICHALZIK R. [Ed.], *VCSELS: Fundamentals, Technology and Applications of Vertical-Cavity Surface-Emitting Lasers*, Springer Series in Optical Sciences, Vol. 166, Springer, Berlin, Heidelberg, 2013, DOI: [10.1007/978-3-642-24986-0](https://doi.org/10.1007/978-3-642-24986-0).
- [8] NING C.Z., *What is laser threshold?*, IEEE Journal of Selected Topics in Quantum Electronics **19**(4), 2013, article 1503604, DOI: [10.1109/JSTQE.2013.2259222](https://doi.org/10.1109/JSTQE.2013.2259222).
- [9] SHIN J.H., JU Y.G., SHIN H.E., LEE Y.H., *Spontaneous emission factor of oxidized vertical-cavity surface-emitting lasers from the measured below-threshold cavity loss*, Applied Physics Letters **70**(18), 1997, pp. 2344–2346, DOI: [10.1063/1.118869](https://doi.org/10.1063/1.118869).
- [10] PAOLI T., *Saturation behavior of the spontaneous emission from double-heterostructure junction lasers operating high above threshold*, IEEE Journal of Quantum Electronics **9**(2), 1973, pp. 267–272, DOI: [10.1109/JQE.1973.1077481](https://doi.org/10.1109/JQE.1973.1077481).
- [11] MIYAMOTO T., SUDA Y., *Simultaneous use of spontaneous emission light in VCSEL for improving efficiency of optical wireless power transmission*, 2018 IEEE International Semiconductor Laser Conference (ISLC), 2018, pp. 1–2, DOI: [10.1109/ISLC.2018.8516233](https://doi.org/10.1109/ISLC.2018.8516233).
- [12] WU J., LONG H., SHI X., YING L., ZHENG Z., ZHANG B., *Reduction of lasing threshold of GaN-based vertical-cavity surface-emitting lasers by using short cavity lengths*, IEEE Transactions on Electron Devices **65**(6), 2018, pp. 2504–2508, DOI: [10.1109/TED.2018.2825992](https://doi.org/10.1109/TED.2018.2825992).
- [13] LEE J.H., MOON J.H., SU P.C., LEE S.H., *Numerical analysis of injected current effects on thermal characteristics of vertical-cavity surface-emitting laser*, Journal of Mechanical Science and Technology **32**(3), 2018, pp. 1463–1469, DOI: [10.1007/s12206-018-0250-5](https://doi.org/10.1007/s12206-018-0250-5).
- [14] MOSER P., LOTT J.A., LARISCH G., BIMBERG D., *Impact of the oxide-aperture diameter on the energy efficiency, bandwidth, and temperature stability of 980-nm VCSELS*, Journal of Lightwave Technology **33**(4), 2015, pp. 825–831, DOI: [10.1109/JLT.2014.2365237](https://doi.org/10.1109/JLT.2014.2365237).

*Received October 16, 2019  
in revised form February 13, 2020*